Efficiency of Thermionic Emission from C_{60}

Rongping Deng and Olof Echt*

Department of Physics, University of New Hampshire, Durham, New Hampshire 03824-3016

Received: January 7, 1998; In Final Form: February 17, 1998

We have determined the number of delayed electrons emitted from an ensemble of gas-phase C_{60}, excited at 355 nm with light from an unfocused pulsed Nd:YAG laser. Delayed electrons are detected by single particle counting and integrated over a time interval of 0.1 μs $\leq t \leq$ 80 μs. At low laser fluence I, the electron number scales as I^p with $p = 6.0 \pm 0.4$. It approaches saturation at a maximum laser fluence of 100 mJ/cm^2, equivalent to a power density of 14 MW/cm^2, where delayed electron emission reaches a probability of 2.6 $\pm$ 1.1% per multiphoton-excited C_{60}. This experimental value is interpreted as a lower limit to the quantum efficiency for electron emission from C_{60}; it provides an upper limit to the efficiency of competing reactions such as dissociation of C_{60} into $C_{58} + C_2$. The dependence of the electron number on the temperature of the fullerene source is in good agreement with the number density of C_{60} in the molecular beam, as computed from published equilibrium vapor pressures.

Introduction

Highly excited gas-phase fullerenes have been observed to emit delayed electrons,[1−11] a continuous spectrum of photons,[12−14] and C_2 fragments.[3,15−23] These phenomena are commonly interpreted as the molecular analogues of thermionic emission,[24] thermal (blackbody-like) radiation,[14,25] and evaporation[26,27] because they occur under conditions where the excitation energy, estimated to range from roughly 15 to 60 eV, is likely to be randomized over all internal degrees of freedom.[28,29] The degree to which they compete with each other is not well-known; neither their absolute nor their relative rates have been determined so far.[30] The experimentalist trying to measure absolute rates for any of these reactions, or relative rates for any pair of them, faces several challenging tasks: controlling the excitation energy of an ensemble of free fullerenes, determining their number, and detecting the products with known efficiencies.

Instead, several reports have been aimed at *estimating* the rates of these reactions and their dependence on the internal excess energy or the effective vibrational temperature.[3,10,17,31−36] These estimates, however, are critically dependent on poorly known or highly controversial quantities: activation energies and frequency factors for thermally activated processes (dissociation, electron emission), emissivities for thermal radiation (for a recent, rigorous calculation of radiative energy loss from C_{60}, see Chupka and Klots;[36] for a general review, see Lifshitz[37]).

Alternatively, one may measure the temporal evolution of a specific reaction. If this is done for an ensemble of fullerenes excited at some time t_0, one can assess whether other, "invisible" reactions contribute significantly, because these would affect the rate of cooling and the evolution of the internal energy distribution as a function of time. For example, dissociation of C_{60}^+ into C_{58}^+ appears to compete with thermal radiation;[38−41] electron emission from neutral[10,11] or negatively[42] charged C_{60} competes with dissociation and radiation, respectively. From these data one can estimate the degree of competition and thereby gain valuable information about the "dark" channels.[10,11,38,39,41,43] However, a less indirect procedure would be highly desirable.

In this contribution we describe a direct measurement of the probability of delayed electron emission from photoexcited fullerenes. A preliminary summary has been published recently.[23] We count the number of delayed electrons emitted after excitation at 355 nm, for a variety of C_{60} number densities (source temperatures) and laser intensities. The number density of C_{60} in the molecular beam is determined by measuring the mass flux density using a quartz microbalance; the interaction volume is defined by collimating the fullerene beam and the unfocused laser beam. Linearity of detector response is examined by varying the source temperature. Over a wide range of temperatures the number of delayed electrons varies, indeed, as the number density of C_{60} in the beam, calculated from published vapor pressures of C_{60}.[44] At lowest laser fluence I, the electron number increases steeply as I^p, with $p = 6.0 \pm 0.4$. At a fluence of 100 mJ/cm^2 the number of delayed electrons per multiphoton-excited C_{60} reaches an approximately constant value of 2.6 $\pm$ 1.1%. This represents a lower limit to the total, time-integrated emission probability. For example, the collection efficiency for electrons emitted several tens of microseconds after the laser pulse is probably less than 100%, and electrons emitted more than 80 μs after the laser pulse are not counted at all.

Experiment

A crossed-beam arrangement (Figure 1) is employed to collect prompt and delayed photoelectrons with what is believed to be near 100% efficiency, at least for delays below 10 μs. A beam of C_{60} (MER, purity 99.5%) emerges from a resistively heated copper cell (orifice diameter 1.4 mm, temperatures ranging from 300 to 500 °C). At a distance of about 30 cm, shortly before intersection with a pulsed beam from a Nd:YAG laser, the low-density molecular beam is collimated by a rectangular slit of 2.0 mm width and 5.0 mm length (measured parallel and orthogonal to the laser beam, respectively). The third harmonic of the unfocused laser beam (355 nm, diameter 6 mm, pulse

* To whom correspondence should be addressed: e-mail OLOF.ECHT@UNH.EDU; Tel (603) 862-3548; fax -2998.

S1089-5639(98)00704-X CCC: $15.00
Published on Web 03/19/1998

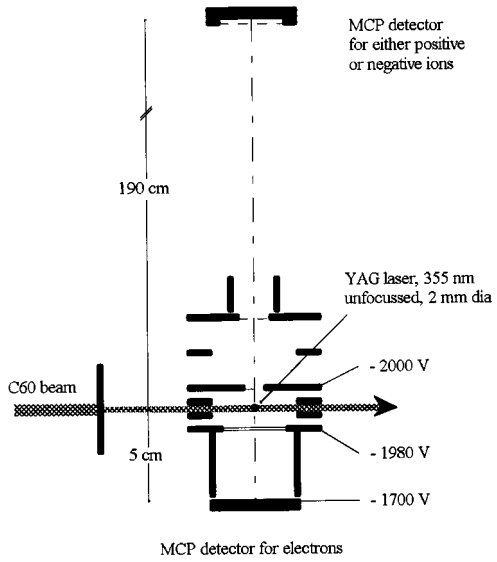

Figure 1. Experimental setup.

duration about 7 ns, repetition rate 50 Hz) is collimated by a circular aperture. Apertures of either 1.0, 2.0, or 4.0 mm diameter are used to keep the detector count rate within a narrow range (see discussion of detector response further below). For ease of comparison, electron count rates quoted in the following are consistently scaled to a laser beam diameter of 2.0 mm.

Photoelectrons are extracted by a weak electric field (10 V/cm) into a short drift tube of 4 cm length; at its end they impinge with a kinetic energy of 300 eV on a microchannelplate detector (MCP, Hamamatsu model 1552-21S, 2.7 cm effective diameter). A homogeneous static magnetic field, generated by Helmholtz coils external to the vacuum chamber, helps to guide photoelectrons to the detector as long as the electron-emitting species have not moved by more than about 1.3 cm along the direction of the molecular beam. At the same time, the magnetic field suppresses electrons originating from other regions of the spectrometer, such as electrons emitted from electrodes hit by scattered laser light. Another drift tube of 190 cm length, antiparallel to the one discussed above, may be used to determine the size distributions of prompt or delayed cations and anions.[23]

To determine the electron emission probability per photoexcited C_{60}, we need to know the number density of C_{60} in the interaction region with the laser beam. This quantity depends on source temperature, orifice diameter and geometry, and the vapor pressure in the source. All of these parameters carry significant uncertainties; published equilibrium vapor pressures of C_{60} disagree by as much as an order of magnitude.[44] We avoid these uncertainties altogether by using a quartz microbalance to determine the mass flux density of the (uncollimated) beam of C_{60} emerging from a carefully outgassed source kept at 460 °C. The flux density is corrected for differences in the distances of source-to-microbalance and source-to-laser beam. Converting the flux density to a number density does require knowledge of the flow velocity, but now the source temperature enters only through its inverse square root; temperature errors of a few degrees will be insignificant.[45] For a source temperature of 460 °C we obtain a C_{60} number density of $n_0 = 1.11 \times 10^7$ cm^{-3} with an estimated error of 10%, equivalent to an equivalent vapor pressure (at room temperature) of 3.5×10^{-10} Torr. We note that the use of a quartz microbalance would underestimate the beam flux if the sticking coefficient of C_{60} were less than one. However, a lower limit of 0.85 has been established experimentally.[46]

The number of photoexcited C_{60} is the product of their number density and the cylindrical interaction volume. However, after completion of the experiments the C_{60} deposit on the 2.0 by 5.0 mm collimator slit was visually inspected, and a significant misalignment was noted between the circular profile of the precollimated fullerene beam (diameter 4 mm) and the slit. Hence, the effective slit width is taken as 1.3 ± 0.4 mm instead of 2.0 mm, equivalent to an interaction volume of 4.1 ± 1.3 mm^3.

The MCP detector is operated in single-particle counting mode: The signal passes through a preamplifier (gain of 10) into a discriminator (detection limit −10 mV) with bandwidths of 300 MHz. Time-of-arrival spectra are accumulated in a time-to-digital converter (TDC) with 20 ns bin width, about 2 bins dead time, and multihit capacity. Spectra are acquired for 100−1000 s. This system is well-suited for low count rate applications. However, peak count rates exceeding ≈0.1 per laser shot and bin (equivalent to 5 MHz) will lead to noticeable spectral distortions because of dead time effects in the electronics and the TDC. At very high event rates, the gain of the detector will drop due to temporal reduction of the high voltage, and an increasing fraction of events will fall below the discriminator threshold. We have analyzed this effect by recording single-shot spectra with a digital oscilloscope. A drop in gain (i.e., a decrease in the amplitude of single events) is clearly discernible at very high peak count rates (≫100 MHz near $t = 0$), and this reduction extends into the later, low count rate part of the spectrum. Excessive peak count rates were avoided as much as possible by reducing either the laser beam diameter, or the source temperature, or the laser pulse energy.

A lower limit to the acceptable count rate is set by the background rate of $<10^{-7}$ counts per laser shot and bin, measured with the laser beam blocked. This value corresponds to a total of only 0.005 counts per bin after an acquisition time of 1000 s. We digitally average the spectra to extract these small numbers: Beyond a delay of $t = 2$ μs, Δn adjacent bins are combined to obtain an average count rate per 20 ns, assigned to a time $t = 0.02\langle n\rangle$ μs, where $\langle n\rangle$ is the average bin address.[47] The number Δn, which may be a noninteger, is determined by the relation $\Delta n/\langle n\rangle = \Delta t/t = 1/100$. Hence, for a delay of 100 μs we average over $\Delta t = 1$ μs, or $\Delta n = 50$ bins, making count rates as low as 10^{-6} per laser shot and bin detectable. The procedure will limit the time resolution, but features with $\Delta t/t \leq 1/100$ neither are expected for delayed electrons nor were observed in any of the nonaveraged spectra.

However, spectral distortions were initially encountered due to the presence of C_n anions and cations, the latter being accelerated away from the detector. They may, however, hit electrodes and release secondary electrons which are then accelerated toward the MCP. Our solution was to reduce the extraction field to 10 V/cm, thus limiting the kinetic energy of positive ions within the ion extraction region. Furthermore, the kinetic energy of electrons and anions is only 300 eV when they hit the MCP. This is near the optimum energy for electron detection but way below the optimum energy for detection of ions. Under these conditions, the calculated total time-of-flight for electrons is about 20 ns. In the present study, the detection of quasi-prompt electrons defines $t = 0$.

According to data sheets for microchannel plate detectors, their detection efficiency for electrons of 300 eV is about 70 ± 10%.[48] This assumes that the average output voltage for "real" events is well above the electronic noise level and also well above the discriminator threshold. To test whether our setup complied with these conditions, we recorded a series of spectra

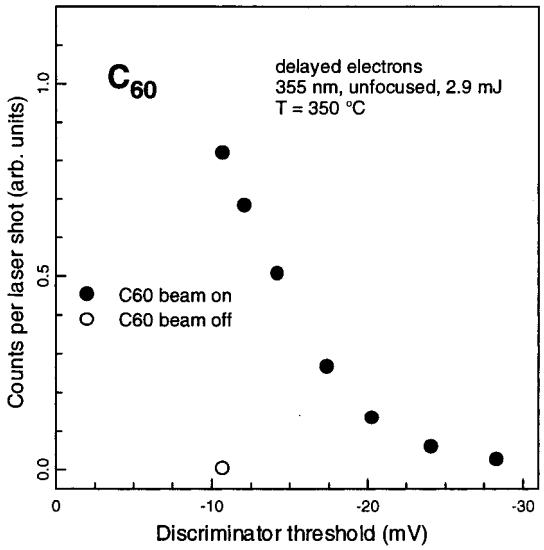

Figure 2. Dependence of electron count rate (arbitrary units) on discriminator threshold. These data suggest that the detection efficiency is limited by the discriminator threshold, even at −10 mV.

with different discriminator thresholds. Results are compiled in Figure 2. The signal-to-noise ratio was excellent for all discriminator thresholds. However, even using the lowest possible trigger threshold of (negative) 10 mV, we observe a strong, continuous decrease of electron count rate with increasing threshold. This suggests that the detection efficiency of our system (MCP + preamplifier + discriminator) was less than optimum. We cannot, however, quantify this loss (relative to the specified value of 70%); hence, no attempt will be made to correct our data for this effect.

The laser pulse energy is measured with a thermopile sensor after the beam exits the vacuum chamber. Values quoted in this study are therefore about 10% less than the actual values in the interaction region. Also, they present time averages; a fast photodiode indicates shot-to-shot fluctuations of 5−10%. Quartz plates, 1.6 mm thick, are inserted into the beam under 45°; they attenuate the laser beam without changing its spatial profile. Spectra discussed in this study were acquired with laser fluences ranging from about 20 to 100 mJ/cm^2 (corresponding to flux densities of 3−14 MW/cm^2 or pulse energies of 0.6−3 mJ for a laser beam diameter of 2.0 mm), except for a few spectra recorded with a mildly focused laser beam.

Results

Figure 3 displays a few representative electron spectra on a semilogarithmic scale. Three spectra, recorded at a source temperature of 370 °C (solid symbols), demonstrate that a change of laser fluence merely changes the overall electron intensity by some factor, but it does not affect their time dependence. This holds true as long as the peak electron intensity stays below about 0.1 events per time bin (20 ns), a condition which sets limits to laser fluence, laser beam diameter, or source temperature. In other words, undistorted spectra at maximum laser fluence require source temperatures well below the one at which the C_{60} number density was established using the quartz microbalance. Connection to that temperature (460 °C) is made by recording several spectra with varying laser fluence at each of eight different source temperatures, ranging from 300 to 500 °C. Details will be discussed further below.

Figure 3 also displays another spectrum, recorded at low laser fluence and with the fullerene beam being blocked by a

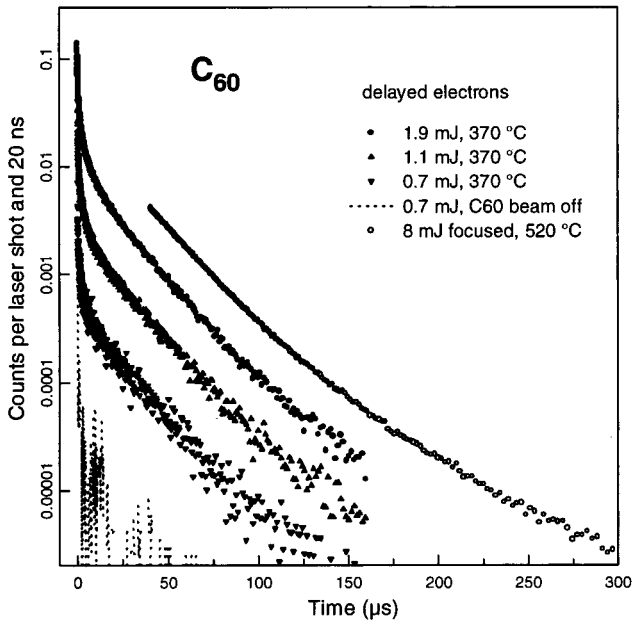

Figure 3. Solid symbols: representative set of delayed electron spectra, recorded for identical source conditions, $T = 370$ °C, but different laser pulse energies. Note the very weak background intensity (dotted line), recorded with the C_{60} beam being blocked. The spectrum recorded at 520 °C with a mildly focused laser (open circles, arbitrary intensity scale) reveals electron emission over at least 300 μs.

mechanical shutter. This "background spectrum" demonstrates that photons, prompt photoelectrons from background gas, or photoelectrons generated at surfaces do not contribute significantly. This is true except for source temperatures $T \leq 300$ °C or for high laser fluence. At maximum laser intensity, the early part of the spectrum does become distorted, and this part has to be excluded from the data analysis. Spectra taken at a laser wavelength of 266 nm did suffer from a significantly larger background; therefore, the present analysis is restricted to data recorded at 355 nm.

The truncated spectrum shown in Figure 3 (open symbols) was recorded with a mildly focused laser at a source temperature of 520 °C. It is displayed here, with its intensity being scaled by an arbitrary factor, to demonstrate that electron emission extends over a delay of, at least, 300 μs.

The total number of electrons emitted from the ensemble of C_{60} per laser shot is most clearly discernible by integrating from the onset of the electron signal[47] to time t. A representative set of data, based on raw spectra recorded at a source temperature $T = 370$ °C (cf. Figure 3), is displayed in Figure 4. Several features are noteworthy: (i) The cumulative intensity increases roughly linearly from 0.1 to 10 μs; i.e., it follows a power law in time. However, after several tens of microseconds it reaches a constant value. (ii) The total number of electrons (i.e., the cumulative intensity collected after $t \approx 100$ μs) increases with increasing fluence from 0.7 to 25 per laser shot. (iii) The cumulative intensity during the first 20−40 ns, which includes all prompt electrons, is less than the total number by nearly 2 orders of magnitude. This is true for low to medium laser fluences. At high laser fluences the early parts of the spectra do become distorted; hence, we cannot assess the relative fraction of prompt electrons.

We extract the number of delayed electrons per laser shot from the unprocessed spectra (as measured by the TDC) by integrating their intensity over a range $0.1 \leq t \leq 80$ μs, thus safely excluding any prompt electrons. Those spectra that do show mild distortions during the first 1−2 μs due to high count

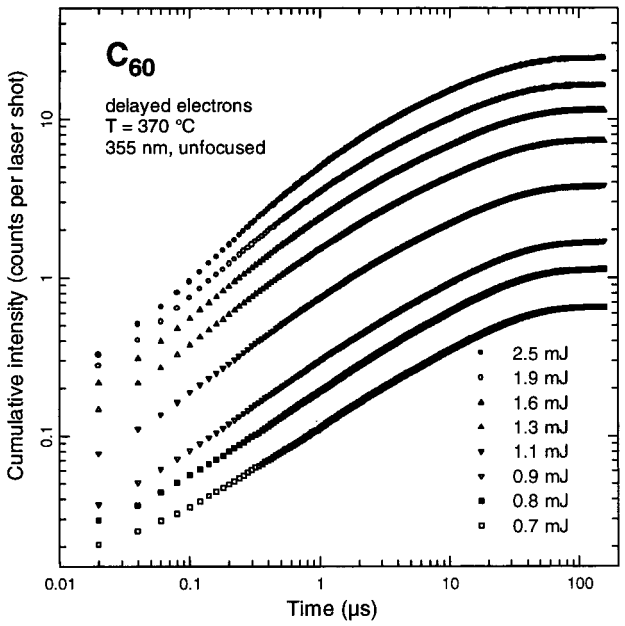

Figure 4. Cumulative number of electrons per laser shot, obtained from spectra like those shown in Figure 3 by integrating over time from time zero to *t*. Note the relatively small fraction of quasi-prompt electrons emitted during the first 20−40 ns.

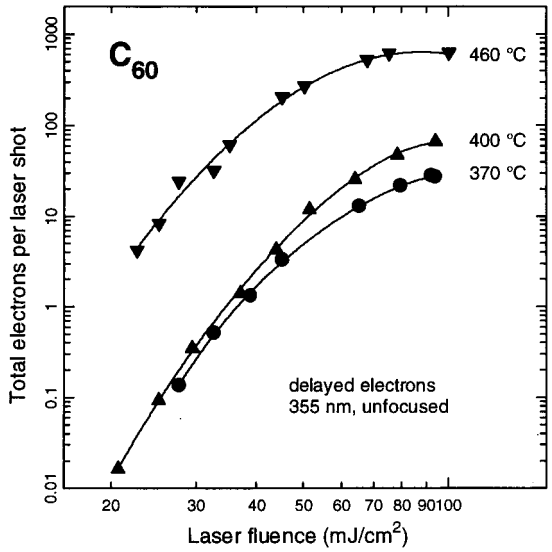

Figure 5. Number of delayed electrons per laser shot, integrated over time intervals 0.1 $\mu s \leq t \leq 80$ μs, as a function of laser fluence, for three different source temperatures.

rates (high laser fluence *and* high source temperature) are integrated over a narrower time range of $5 \leq t \leq 80$ μs and scaled by comparing with other, distortion-free spectra. Counts are scaled, if necessary, to a laser beam diameter of 2.0 mm.

Figure 5 compiles the dependence of delayed electrons per laser shot on laser fluence, for source temperatures of 370, 400, and 460 °C. For all source temperatures, the curves feature an initial steep slope of 6.0 ± 0.4 while they appear to saturate at maximum laser fluence.

As noted above, the temperature dependence of the electron signal is extracted by comparing pairs of spectra taken at different source temperatures but identical, low laser fluence. This procedure is cumbersome, but this way we can extend the dynamic range of the detector system; we avoid errors due to nonlinearity of the detector output (loss of detection efficiency caused by space charge at the anode, temporal breakdown of

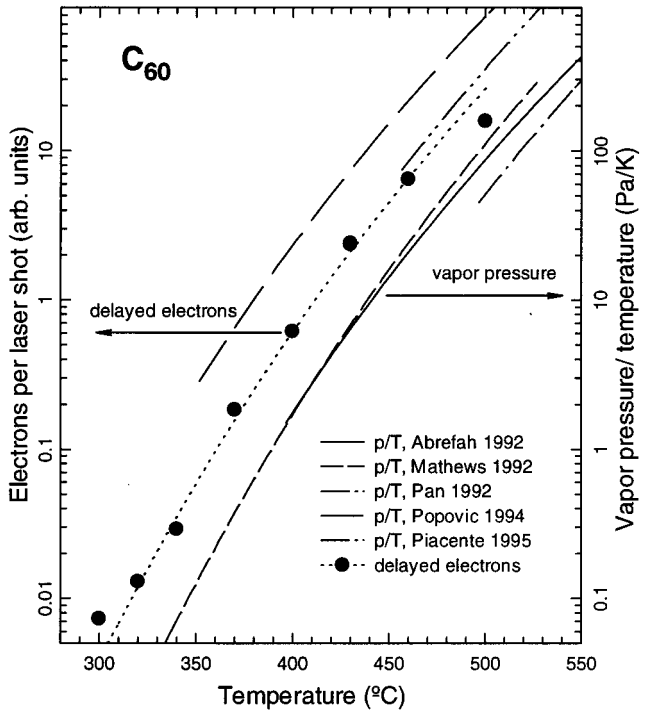

Figure 6. Comparison of the temperature dependence of the number of delayed electrons (full circles, left scale) with the quotient of equilibrium vapor pressure, *p*, and source temperature, *T*. This quotient is linearly related to the number density of C_{60} in the molecular beam. Values for *p* are taken from the literature.[44] A second-law sublimation enthalpy of 168 ± 3 kJ mol^{-1} is derived from our data.

detector voltage, etc.). A summary of this analysis is displayed in Figure 6 which shows the number of electrons (solid circles) on a logarithmic scale (left ordinate, arbitrary units). These data are expected to scale as the number density of C_{60} in the beam, hence as p/T. The vapor pressure curve $p(T)$ has been determined by a number of groups.[44] The lines shown in Figure 6 display published values of p/T (right ordinate, in pascal/kelvin). Analytical expressions have been plotted rather than individual data points; they were either taken from the literature or obtained by least-squares-fitting the reported vapor pressure data. Our electron yield does, indeed, increase linearly with p/T over a wide range of temperatures. This agreement lends credence to the data analysis; it demonstrates that the probability of delayed electron emission is not significantly affected by the source temperature. Deviations near the lower and upper end of the temperature scale are probably caused by insufficient signal-to-background ratio and by detector saturation, respectively. Note that our data extend to lower temperatures than most of the other reported vapor pressure curves. According to our data, the vapor pressure scales with temperature as $\log(p/\text{Pa}) = \text{const} - (8798 \pm 126)/T$ (dotted line in Figure 6). This corresponds to a second-law sublimation enthalpy of 168 ± 3 kJ mol^{-1} for the temperature range $490 \leq T \leq 730$ K. Second-law sublimation enthalpies reported by other researchers range from about 160 to 190 kJ mol^{-1}.[44]

Using the temperature dependence of the beam density (Figure 6), we can combine the asymptotic values of the three data sets shown in Figure 5 to an average total electron number of $N_e = 860 \pm 200$. This value refers to a source temperature of 460 °C, a laser fluence of 100 mJ/cm^2, and integration over 0.1 $\mu s \leq t \leq 80$ μs. We derive the (experimental) probability P_e^{exp} of delayed electron emission per photoexcited C_{60} as follows:

$$P_e^{exp} = N_e/\eta_d n_{C_{60}} V \quad (1)$$

where $\eta_d = 70 \pm 10\%$ is the detection efficiency of the microchannel plate detector for electrons of 300 eV kinetic energy, $n_{C_{60}} = (1.1 \pm 0.1) \times 10^7$ cm^{-3} is the number density of C_{60} in the molecular beam at 460 °C, and $V = 4.1 \pm 1.3$ mm^3 is the interaction volume between the C_{60} beam and the laser beam. We thus obtain a value of $P_e^{exp} = 2.6 \pm 1.1\%$, where the individual uncertainties were combined in quadrature.

Discussion

Let us consider a microcanonical ensemble of C_{60}, prepared at time $t = 0$ with an internal energy ϵ of, roughly, 15−60 eV, supposed to be randomized over all accessible degrees of freedom. Among others, the following decay channels will be open:

$$C_{60}(\epsilon) \xrightarrow{k_{e^-}} C_{60}^+ + e^- \quad (2a)$$

$$C_{60}(\epsilon) \xrightarrow{k_{C_2}} C_{58} + C_2 \quad (2b)$$

$$C_{60}(\epsilon) \xrightarrow{k_\nu} C_{60} + h\nu \quad (2c)$$

One may characterize the relative or absolute efficiencies of thermionic emission (2a), evaporation (2b), and thermal radiation (2c) by referring to their corresponding rates k_i which will, of course, depend on the energy ϵ. Moreover, these rates will be time-dependent because the ensemble of C_{60} will gradually cool through thermal radiation.

Alternatively, we may characterize the efficiency by the probability P_i for a reaction to occur within some time interval $t_1 \le t \le t_2$, normalized to the number of excited C_{60} being present at time zero, $N_{C_{60}}(t{=}0)$. The relation between P_e and the electron emission rate k_e is, by definition,

$$P_e(\epsilon,t_1,t_2) = \frac{1}{N_{C_{60}}(t{=}0)} \int_{t_1}^{t_2} N_{C_{60}}(t)\, k_e(\epsilon(t))\, dt \quad (3)$$

If the integral is extended from $t = 0$ to $t = \infty$, P_e represents the *quantum efficiency* $\eta_e(\epsilon)$ for electron emission from C_{60}. In principle, this quantity would be unity if all other reaction channels were negligible, provided ϵ exceeds the ionization energy. In practice, radiative cooling will be important (i.e., nonnegligible compared to k_e) at low excitation because of its nonexponential dependence on temperature.[10,35−40,49] At the other end of the energy scale, for ϵ exceeding 70−80 eV,[22,50] additional decay channels such as fission-like dissociation or nonstatistical fragmentation into small carbon clusters are accessible, thus reducing $N_{C_{60}}(t)$. Somewhere in between, where the main competing process is, presumably, C_2 emission, the quantum efficiency $\eta_e(\epsilon)$ will reach a maximum value, η_e^{max}, for which our experiment provides a rigorous lower limit:

$$P_e^{exp} = 2.6 \pm 1.1\% \le P_e(\epsilon, 0.1\,\mu s, 80\,\mu s) < P_e(\epsilon, 0, \infty) \equiv \eta_e(\epsilon) \le \eta_e^{max} \quad (4)$$

For the following reasons, our experimental value is merely a lower limit to η_e^{max}:

1. We have integrated the electron signal over a finite time interval, $0.1\ \mu s \le t \le 80\ \mu s$. Excluding times below 0.1 μs does not appear to cause a significant error (see Figure 4), but the number of electrons that will be emitted after more than 80 μs is unknown. The disparity between $P_e(\epsilon, 0.1\ \mu s, 80\ \mu s)$ and $P_e(\epsilon, 0, \infty)$ will, of course, be strongest at low excitation energy, where the lifetime with respect to electron emission, $1/k_e$, greatly exceeds the upper limit of the integral in eq 3.

2. We have assumed that the collection efficiency for delayed electrons emitted during $0.1\ \mu s \le t \le 80\ \mu s$ is 100%. This is probably a valid estimate for short delays, thanks to the electrostatic extraction field and the magnetic guiding field. However, at a source temperature of 460 °C the neutral fullerenes move with an average flow velocity of 173 m/s.[45] They move parallel to the detector surface; electrons emitted tens of microseconds after the laser pulse will not be mapped onto the detector with 100% efficiency. We have not attempted to correct our spectra for this loss because the uncertainties would be too large.

3. We have not prepared a microcanonical ensemble of C_{60}. Therefore, even if radiative cooling were negligible, the average energy $\langle\epsilon\rangle$ of the ensemble will gradually drop because highly excited C_{60} will decay into C_{58} or C_{60}^+ more quickly than colder species.[26]

4. We have not been able to increase the laser fluence beyond 100 mJ/cm^2; saturation is suggested by the data in Figure 5, but not proven.

5. The detector efficiency was taken to be 70 ± 10% as specified in data sheets for this type of detector. However, the count rate recorded as a function of discriminator threshold (see Figure 2) indicated that our threshold was somewhat high, probably resulting in a reduced detector efficiency (see Experimental Section).

6. At high laser fluence, prompt destruction of fullerenes may become substantial. The experiment will therefore overestimate the number density of photoexcited C_{60} in eq 1.

To illustrate the last point, we plot time-of-flight mass spectra of fullerene cations in Figure 7 (for details, see ref 23). The lower and middle traces are representative of the conditions under which electron spectra were recorded (unfocused laser,

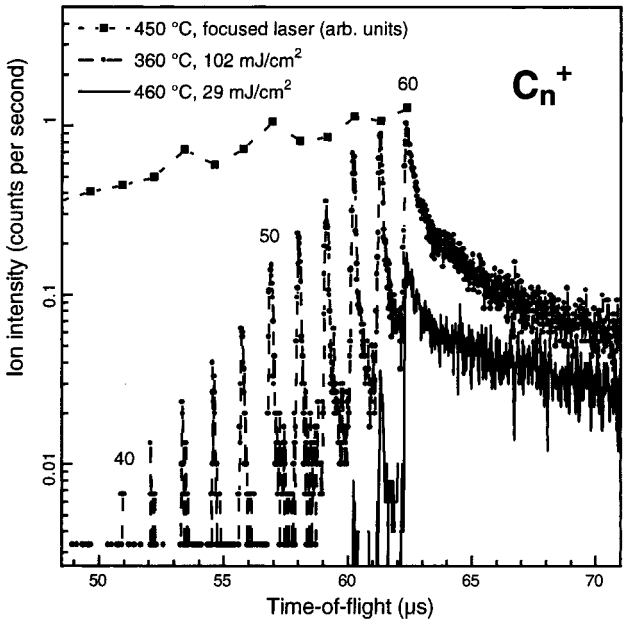

Figure 7. Time-of-flight mass spectra of fullerenes, ionized by multiphoton excitation at 355 nm. The lower and middle traces were recorded with an unfocused laser at fluences of 29 and 102 mJ/cm^2, respectively; they are representative of the conditions chosen for collection of delayed electrons. The solid squares represent the size distribution of fullerene fragment ions recorded with much higher fluence (focused laser).

wavelength 355 nm, fluence 29 and 102 mJ/cm^2, respectively). At low fluence, the only observable fragments are C_{58}^+ and C_{56}^+; the peak intensities of smaller fragment ions are less than 1% of that of C_{60}^+. At a maximum fluence of 102 mJ/cm^2, fragmentation is much more pronounced. The total (time-integrated) number of fullerene fragment ions (size $40 \leq n \leq 58$) reaches 30% of the total C_{60}^+ intensity, integrated from the quasi-prompt peak at 62 μs to the end of the spectrum at 82 μs, thus including any C_{60} ions formed with a delay of $\leq$20 μs. However, small carbon fragments ions ($n < 30$) are not yet observed; their peak intensities are, at most, 0.5% of C_{60}^+. Also, note that these size distributions of cations may underestimate the extent of fragmentation, because neutral species such as those resulting from reaction 2b go undetected. They have been identified by one-photon ionization in the VUV[18,51,52] and fluorescence[20,53] and reionization,[54] but their yield relative to that of C_{60}^+, and its dependence on laser fluence, remains unknown.

At considerably higher fluence, accomplished by mildly focusing the laser beam, we observe fullerene fragment ions with peak intensities close to that of C_{60}^+ (see Figure 7, solid squares). Their total intensity, integrated from $40 \leq n \leq 58$, now approaches that of C_{60}^+ (integrated from 62 μs $\leq t \leq$ 82 μs). At the same time, small carbon cluster ions are abundant; their integrated intensity ($1 \leq n \leq 30$) is about 25% of the integrated C_{60}^+ intensity. These examples suggest that saturation of the delayed electron signal does, indeed, correlate with the onset of strong fragmentation.

We have maintained that our experimental value, $P_e^{exp} = 2.6 \pm 1.1\%$, establishes a rigorous lower bound to the quantum efficiency η_e^{max}. The following effects may actually lead to an *overestimate* of the total electron number, but these potential errors are small:

1. We may have underestimated the beam density of fullerenes by assuming a sticking coefficient of 100%, but by no more than 18%. A lower limit of 85% has been established experimentally.[46]

2. We may have underestimated the efficiency for detection of electrons at the microchannel plate for which a value of 70 $\pm$ 10% was assumed, but by no more than 25%.

3. We may have counted delayed electrons originating from species other that C_{60}, such as C_{60}^+, C_{58}, or small carbon fragments. However, mass analysis of delayed cations[6] shows that, under laser irradiation conditions such as those used in the present study, fullerene fragment ions C_{58}^+, C_{56}^+, etc., form with much lower intensity than C_{60}^+. This is also evident from time-of-flight mass spectra; see Figure 7. Delayed formation of multiply charged fullerenes from C_{60}^+ (or smaller cations) is exceedingly unlikely because of the increased ionization energies of cations.[37,55,56] Small carbon fragments (fewer than 30 atoms) do not show any sign of delayed ionization.[6]

4. Oscillations in the amplifier output and cable reflections may, in principle, result in individual electrons being counted more than once. We have verified that this does not happen, by deliberately introducing additional dead time into the discriminator circuit and by comparing "single shot" spectra at the amplifier output (= discriminator input) with the output of the discriminator, using a fast digital oscilloscope. Therefore, our experimental value is, within its specified uncertainty, a valid lower limit to the quantum efficiency for delayed electron emission. It provides an approximate upper limit for the relative rates of competing dissociative channels:

$$k_e/[k_e + \sum k_d] \geq 0.026 \qquad (5)$$

where the sum extends over all dissociative channels. This simplifies, if C_2 loss is dominant, to

$$k_{C_2} \leq k_e/0.026 \approx 40k_e \qquad (6)$$

Circumstantial evidence for the efficient competition of thermionic emission with dissociation had been reported earlier.[8,35,37] So far, however, no direct, quantitative information has been available. Relations 5 and 6 are only approximate, because neither the number of excited C_{60} nor their internal energy (or energy distribution) is strictly constant during the interval of integration in eq 3. Nevertheless, it may be applied to test the validity of reaction rates published in the literature. For example, Kolodney et al.[38] have reported an Arrhenius activation energy of 4.4 $\pm$ 0.1 eV and a preexponential factor $A = 2.5 \times 10^{13}$ s^{-1} for dissociation of C_{60}. If we assume that the rate of electron emission is appropriately described by an Arrhenius expression with an ionization energy[37,57] of 7.6 eV and a preexponential factor[32] of 1.9×10^{16} s^{-1}, then eq 6 will be violated unless the effective temperature of C_{60} is high enough to support dissociation rates exceeding 2×10^7 s^{-1} and, therefore, electron emission rates exceeding 5×10^5 s^{-1}. This scenario is hardly consistent with our data which reveal (Figure 4) that a substantial fraction of delayed electrons is emitted with a delay exceeding some 10 μs. Several other estimates of the dissociation rate[3,10,17,31,35] are, however, not inconsistent with the limit set by eq 6. While dissociation energies are often reported with amazingly small errors, the corresponding preexponential factors (or, in RRKM language, the nature of the transition state) carry sufficiently large uncertainties such that dissociation energies in the range 6$-$8 eV can be made to comply with eq 6. However, a definitive lower limit for the dissociation energy cannot be derived from our data, because no clear-cut lower limit is known for the preexponential factor.

We emphasize that our data do not provide an *upper* bound to the efficiency of thermionic emission, although it may be derived indirectly. Hansen and Echt[11] have noted that the electron yield (Figure 3) follows a power law in time, $I_e(t) = \text{const} \times t^{-q}$. The value of the exponent q, though, is significantly less than 1.0. This was attributed to competition with dissociation (reaction 2b), for which an activation energy of 11.9 $\pm$ 1.9 eV could thus be derived. This value is significantly higher than most other experimental values, but it agrees closely with theoretical values (for a recent compilation of dissociation energies of C_{60}^+, see ref 58). In the analysis it had to be assumed that the rate of dissociation exceeds that of electron emission by an order of magnitude, at least. This implies that the preexponential factor of dissociation exceeds that of electron emission by several orders of magnitude. The conclusion disagrees with preexponentials derived by Klots,[32,33] but it is consistent with results obtained when both reactions are treated by detailed balance.[59]

Conclusion

On the basis of a direct count of delayed electrons emitted per photoexcited C_{60}, we have derived a lower limit to the quantum efficiency for delayed electron emission from photoexcited C_{60}, $\eta_e^{max} \geq 2.6 \pm 1.1\%$. The maximum quantum efficiency would pertain to a microcanonical ensemble characterized by excitation energies that are sufficiently high such that radiative cooling only plays a minor role but sufficiently low to render ineffective all dissociation channels that feature activation energies higher than C_2 loss. In this intermediate energy range, our lower bound to η_e^{max} will translate to an

approximate upper limit for the rate of dissociation, $k_{C_2} \leq 40k_e$. The relation argues against low dissociation energies unless these are combined with unusually small preexponential factors.

Acknowledgment. This material is based upon work supported by the National Science Foundation under Grant PHY-9507959.

References and Notes

(1) Campbell, E. E. B.; Ulmer, G.; Hertel, I. V. *Phys. Rev. Lett.* **1991**, *67*, 1986. Campbell, E. E. B.; Ulmer, G.; Hertel, I. V. *Z. Phys. D* **1992**, *24*, 81.

(2) Wurz, P.; Lykke, K. R. *J. Chem. Phys.* **1991**, *95*, 7008.

(3) Wurz, P.; Lykke, K. R. *J. Phys. Chem.* **1992**, *96*, 10129.

(4) Yeretzian, C.; Whetten, R. L. *Z. Phys. D* **1992**, *24*, 199.

(5) Walder, G.; Echt, O. *Int. J. Mod. Phys. B* **1992**, *6*, 3881.

(6) Walder, G.; Kennedy, K. W.; Echt, O. *Z. Phys. D* **1993**, *26*, S288.

(7) Ding, D.; Compton, R. N.; Haufler, R. E.; Klots, C. E. *J. Phys. Chem.* **1993**, *97*, 2500.

(8) Ding, D.; Huang, J.; Compton, R. N.; Klots, C. E.; Haufler, R. E. *Phys. Rev. Lett.* **1994**, *73*, 1084.

(9) Vostrikov, A. A.; Dubov, D. Y.; Agarkov, A. A. *Tech. Phys. Lett.* **1995**, *21*, 715.

(10) Weis, P.; Rockenberger, J.; Beck, R. D.; Kappes, M. M. *J. Chem. Phys.* **1996**, *104*, 3629.

(11) Hansen, K.; Echt, O. *Phys. Rev. Lett.* **1997**, *78*, 2337.

(12) Rohlfing, E. A.; Chandler, D. W. *Chem. Phys. Lett.* **1990**, *170*, 44.

(13) Mitzner, R.; Campbell, E. E. B. *J. Chem. Phys.* **1995**, *103*, 2445.

(14) Vostrikov, A. A.; Dubov, D. Y.; Agarkov, A. A. *JETP Lett.* **1996**, *63*, 963.

(15) O'Brien, S. C.; Heath, J. R.; Curl, R. F.; Smalley, R. E. *J. Chem. Phys.* **1988**, *88*, 220.

(16) Hohmann, H.; Callegari, C.; Furrer, S.; Grosenick, D.; Campbell, E. E. B.; Hertel, I. V. *Phys. Rev. Lett.* **1994**, *73*, 1919. Hohmann, H.; Ehlich, R.; Furrer, S.; Kittelmann, O.; Ringling, J.; Campbell, E. E. B. *Z. Phys. D* **1995**, *33*, 143.

(17) Foltin, M.; Lezius, M.; Scheier, P.; Märk, T. D. *J. Chem. Phys.* **1993**, *98*, 9624.

(18) Lykke, K. R. *Phys. Rev. A* **1995**, *52*, 1354.

(19) Scheier, P.; Dünser, B.; Wörgötter, R.; Muigg, D.; Matt, S.; Echt, O.; Foltin, M.; Märk, T. D. *Phys. Rev. Lett.* **1996**, *77*, 2654. Foltin, M.; Echt, O.; Scheier, P.; Dünser, B.; Wörgötter, R.; Muigg, D.; Matt, S.; Märk, T. D. *J. Chem. Phys.* **1997**, *107*, 6246.

(20) Heszler, P.; Carlsson, J. O.; Demirev, P. *Phys. Rev. B* **1996**, *53*, 12541.

(21) Dünser, B.; Echt, O.; Scheier, P.; Märk, T. D. *Phys. Rev. Lett.* **1997**, *79*, 3861.

(22) Beck, R. D.; Rockenberger, J.; Weis, P.; Kappes, M. M. *J. Chem. Phys.* **1996**, *104*, 3638.

(23) Deng, R.; Littlefield, G.; Echt, O. *Z. Phys. D* **1997**, *40*, 355.

(24) Klots, C. E.; Compton, R. N. *Surf. Rev. Lett.* **1996**, *3*, 535.

(25) Frenzel, U.; Hammer, U.; Werstje, H.; Kreisle, D. *Z. Phys. D* **1997**, *40*, 108.

(26) Klots, C. E. *J. Phys. Chem.* **1988**, *92*, 5864.

(27) Fröbrich, P. *Ann. Phys.* **1997**, *6*, 403.

(28) For a discussion of nonthermal emission mechanisms for electron emission, see: Jones, A. C.; Dale, M. J.; Banks, M. R.; Gosney, I.; Langridge-Smith, P. R. R. *Mol. Phys.* **1993**, *80*, 583. Loepfe, M.; Siegmann, H. C.; Sattler, K. *Z. Phys. D* **1993**, *26*, S311. Zhang, Y.; Stuke, M. *Phys. Rev. Lett.* **1993**, *70*, 3231. Lykke, K. R. *Phys. Rev. Lett.* **1995**, *75*, 1234. Stuke, M.; Zhang, Y. *Phys. Rev. Lett.* **1995**, *75*, 1235. Klots, C. E.; Compton, R. N. *Phys. Rev. Lett.* **1996**, *76*, 409. Stuke, M.; Zhang, Y. *Phys. Rev. Lett.* **1996**, *76*, 4093. Gallogly, E. B.; Bao, Y. H.; Han, K. L.; Lin, H.; Jackson, W. M. *J. Phys. Chem.* **1994**, *98*, 3121.

(29) For experiments involving C_{60}^- anions which we exclude from our discussion, see: Yeretzian, C.; Hansen, K.; Whetten, R. L. *Science* **1993**, *260*, 652. Yeretzian, C.; Beck, R. D.; Whetten, R. L. *Int. J. Mass Spectrom. Ion Processes* **1994**, *135*, 79. Demirev, P.; Brinkmalm, G.; Eriksson, J.; Papaleo, R.; Hakansson, P.; Sundqvist, B. U. R. *Phys. Rev. B* **1994**, *50*, 9636.

(30) For thermionic emission from atomic clusters other than fullerenes, see: Cartier, S. F.; May, B. D.; Castleman, A. W. *J. Chem. Phys.* **1996**, *104*, 3423. Leisner, T.; Athanassenas, K.; Kreisle, D.; Recknagel, E.; Echt, O. *J. Chem. Phys.* **1993**, *99*, 9670. Collings, B. A.; Amrein, A. H.; Rayner, D. M.; Hackett, P. A. *J. Chem. Phys.* **1993**, *99*, 4174.

(31) Yoo, R. K.; Ruscic, B.; Berkowitz, J. *J. Chem. Phys.* **1992**, *96*, 911.

(32) Klots, C. E. *Chem. Phys. Lett.* **1991**, *186*, 73.

(33) Klots, C. E. *Z. Phys. D* **1991**, *20*, 105.

(34) Sandler, P.; Lifshitz, C.; Klots, C. E. *Chem. Phys. Lett.* **1992**, *200*, 445.

(35) Wan, Z.; Christian, J. F.; Basir, Y.; Anderson, S. L. *J. Chem. Phys.* **1993**, *99*, 5858.

(36) Chupka, W. A.; Klots, C. E. *Int. J. Mass Spectrom. Ion Processes* **1998**, *167/168*, 595.

(37) Lifshitz, C. *Mass Spectrom. Rev.* **1993**, *12*, 261.

(38) Kolodney, E.; Tsipinyuk, B.; Budrevich, A. *J. Chem. Phys.* **1995**, *102*, 9263. Kolodney, E.; Budrevich, A.; Tsipinyuk, B. *Phys. Rev. Lett.* **1995**, *74*, 510.

(39) Hansen, K.; Campbell, E. E. B. *J. Chem. Phys.* **1996**, *104*, 5012.

(40) Laskin, J.; Behm, J. M.; Lykke, K. R.; Lifshitz, C. *Chem. Phys. Lett.* **1996**, *252*, 277.

(41) Laskin, J.; Lifshitz, C. *Chem. Phys. Lett.* **1997**, *277*, 564.

(42) Andersen, J. U.; Brink, C.; Hvelplund, P.; Larsson, M. O.; Nielsen, B. B.; Shen, H. *Phys. Rev. Lett.* **1996**, *77*, 3991.

(43) Hansen, K.; Campbell, E. E. B. *Chem. Phys. Lett.*, in press.

(44) Abrefah, J.; Olander, D. R.; Balooch, M.; Siekhaus, W. J. *Appl. Phys. Lett.* **1992**, *60*, 1313. Mathews, K.; Baba, M. S.; Narasimhan, T. S. L.; Balasubramanian, R.; Sivaraman, N.; Srinivasana, T. G.; Rao, P. R. V. *J. Phys. Chem.* **1992**, *96*, 3566. Korobov, M. V.; Sidorov, L. N. *J. Chem. Thermodyn.* **1994**, *26*, 61. Piacente, V.; Gigli, G.; Scardala, P.; Giustini, A.; Ferro, D. *J. Phys. Chem.* **1995**, *99*, 14052. Popovic, A.; Drazic, G.; Marsel, J. *Rapid Commun. Mass Spectrom.* **1994**, *8*, 985. Popovic, A. *Rapid Commun. Mass Spectrom.* **1996**, *10*, 1433.

(45) Hudson, J. B. *Surface Science;* Butterworth-Heinemann: Boston, MA, 1992.

(46) Maltsev, V. A.; Nerushev, O. A.; Novopashin, S. A.; Selivanov, B. A. *Chem. Phys. Lett.* **1993**, *212*, 480.

(47) In the spectra, time $t = 0$ and bin number zero are assigned to the arrival of quasi-prompt electrons.

(48) Galileo Electro-Optics, data sheet for microchannel plate detectors.

(49) Mitzner, R.; Campbell, E. E. B. *Surf. Rev. Lett.* **1996**, *3*, 759.

(50) Muigg, D.; Scheier, P.; Becker, K.; Märk, T. D. *J. Phys. B* **1996**, *29*, 5193.

(51) Lykke, K. R.; Wurz, P. *J. Phys. Chem.* **1992**, *96*, 3191.

(52) Kaizu, K.; Kohno, M.; Suzuki, S.; Shiromaru, H.; Moriwaki, T.; Achiba, Y. *J. Chem. Phys.* **1997**, *106*, 9954.

(53) Gruen, D. M.; Liu, S. Z.; Krauss, A. R.; Pan, X. Z. *J. Appl. Phys.* **1994**, *75*, 1758.

(54) Polce, M. J.; Beranova, S.; Nold, M. J.; Wesdemiotis, C. *J. Mass Spectrom.* **1996**, *31*, 1073.

(55) Maruyama, S.; Lee, M. Y.; Haufler, R. E.; Chai, Y.; Smalley, R. E. *Z. Phys. D* **1991**, *19*, 409.

(56) Matt, S.; Echt, O.; Wörgötter, R.; Grill, V.; Scheier, P.; Lifshitz, C.; Märk, T. D. *Chem. Phys. Lett.* **1997**, *264*, 149.

(57) deVries, J.; Steger, H.; Kamke, B.; Menzel, C.; Weisser, B.; Kamke, W.; Hertel, I. V. *Chem. Phys. Lett.* **1992**, *188*, 159.

(58) Matt, S.; Echt, O.; Wörgötter, R.; Scheier, P.; Klots, C. E.; Märk, T. D. *Int. J. Mass Spectrom. Ion Processes* **1998**, *167/168*, 753.

(59) Hansen, K.; Echt, O., to be published.